

Long-Wavelength Analysis of Plane Wave Irradiation of an Ellipsoidal Model of Man

HABIB MASSOUDI, MEMBER, IEEE, CARL H. DURNEY, MEMBER, IEEE, AND
CURTIS C. JOHNSON, SENIOR MEMBER, IEEE

Abstract—Expressions are derived for the induced electric fields in an ellipsoidal model of man, and experimental animals irradiated by an electromagnetic (EM) plane wave when the wavelength is long compared to the dimensions of the ellipsoid. Calculations of the power absorbed by an ellipsoidal model of man are given for six different orientations of the ellipsoid with respect to the incident plane wave field vectors. The results show that the induced fields and the absorbed power in the ellipsoid are strong functions of frequency, size, and orientation with respect to the incident EM field vectors. The results for the ellipsoidal model of man are also compared with those of the prolate spheroidal model.

I. INTRODUCTION

A LONG-WAVELENGTH analysis of electromagnetic (EM) plane wave (perturbation technique) has recently been developed and applied to prolate spheroidal models of man and experimental animals [1], [2]. The results of power absorbed calculations in the prolate spheroid models of man and some experimental animals show that orientation of the body with respect to the incident plane wave vectors is an extremely important variable which can make an order-of-magnitude difference in EM power absorption. This strong dependence of EM power absorption upon orientation has also been observed experimentally [3]. Experiments have also been conducted at the School of Aerospace Medicine, Brooks Air Force Base, to measure the EM power absorption in a 70-kg saline-filled prolate spheroidal human phantom, twenty 3.5-kg saline-filled prolate spheroidal monkey phantoms, and twenty live rhesus monkeys [4]. Results of the calculations for spheroidal models have been compared with measurements of power absorbed by saline-filled spheroidal phantoms, and good agreement between calculations and measurements has been found. However, agreement between theory and measurements for live monkeys was not as good as that for prolate spheroidal phantoms [4]. It was found that a significant difference in power absorption occurred when the monkeys were rotated 90° about their long axis. The prolate spheroidal model did not predict this because a prolate spheroid has circular cross sections normal to its long axis, whereas for a monkey, or in general for a primate, cross sections taken normal to the long axis appear more elliptical than circular. A principal conclusion from these comparisons is that an ellipsoidal model will

be a superior representation of primates (man, monkey, and others), and the prolate spheroidal model seems to be adequate only for rodents (mice, rats, and others) since for these species, cross sections taken normal to the long axis appear approximately circular.

In this paper, the perturbation technique, described in [1], is applied to analyze the internal fields in an ellipsoid irradiated by a plane wave for each of the six major orientations of the incident fields with respect to the ellipsoid. Expressions for average absorbed power and power distribution inside the ellipsoid are given. The results of power absorbed calculations in ellipsoidal models of man are compared with those of prolate spheroidal models. Curves of power absorption versus frequency show that the absorbed power is a strong function of size and orientation of the ellipsoid in the incident fields.

II. FIRST-ORDER INTERNAL FIELDS FOR THE ELLIPSOID IRRADIATED BY AN EM PLANE WAVE

In this section the perturbation technique is applied to find the solution of the zeroth- and first-order equations for a plane wave incident on a tissue ellipsoid. The equation of ellipsoid in the rectangular coordinate system is

$$\frac{x^2}{a^2} + \frac{y^2}{b^2} + \frac{z^2}{c^2} = 1$$

where a , b , and c are the semiprincipal axes of the ellipsoid with $a > b > c$.

Expressions for the internal electric fields and the absorbed power are given for each of the six primary polarizations. For convenience in referring to these polarizations, the following definition of polarization is made. The polarization is defined in terms of which of the vectors E^i , H^i , and K are parallel with the three axes of the ellipsoid. (E^i is the incident electric field vector, H^i the magnetic field vector, and K the propagation vector.) The vector parallel to the longest axis is listed first, the one parallel to the next longest axis is listed second, and the one parallel to the shortest axis is listed last. Thus EHK polarization is the one in which the incident electric field vector is parallel to the longest axis (length a), the incident magnetic field vector is parallel to the next longest axis (length b), and the propagation vector is parallel to the shortest axis (length c).

A. Derivations for EKH Polarization

The first polarization considered is EKH polarization. For this polarization $E^i \parallel \hat{x}$ and $H^i \parallel -\hat{z}$. Since the per-

Manuscript received January 7, 1976; revised June 2, 1976. This work was supported by the U.S. Air Force School of Aerospace Medicine, Brooks Air Force Base, TX 78235.

H. Massoudi is with the Department of Electrical Engineering, University of Utah, Salt Lake City, UT 84112.

C. H. Durney is with the Department of Electrical Engineering and Bioengineering, University of Utah, Salt Lake City, UT 84112.

C. C. Johnson is with the Department of Bioengineering, University of Utah, Salt Lake City, UT 84112.

turbation technique has been described in [1], only the outline of the procedure and the results are given here.

1) Each set of incident, internal, and scattered electric and magnetic fields is expanded in a power series of $(-jk)$, where $j = (-1)^{1/2}$ and k is the free-space propagation constant.

2) Equations for the n th-order field terms are obtained by requiring the series expansions of the incident, scattered, and internal fields to satisfy both Maxwell's equations and the boundary conditions.

The results for the internal fields are as follows:

$$\nabla \times \mathbf{E}_0 = 0 \quad (1)$$

$$\nabla \times \mathbf{E}_n = \eta_0 \mathbf{H}_{n-1}, \quad n \geq 1 \quad (2)$$

$$\nabla \times \mathbf{H}_0 = \sigma \mathbf{E}_0 \quad (3)$$

$$\nabla \times \mathbf{H}_n = \sigma \mathbf{E}_n - \frac{\epsilon_r}{\eta_0} \mathbf{E}_{n-1}, \quad n \geq 1 \quad (4)$$

$$\nabla \cdot \mathbf{E}_0 = 0 \quad (5)$$

$$\nabla \cdot \left(\sigma \mathbf{E}_n - \frac{\epsilon_r}{\eta_0} \mathbf{E}_{n-1} \right) = 0, \quad n \geq 1 \quad (6)$$

$$\nabla \cdot \mathbf{H}_n = 0 \quad (7)$$

where $k = \omega \sqrt{\mu_0 \epsilon_0}$, $\epsilon_r = \epsilon/\epsilon_0$ (real), σ is the conductivity of the ellipsoid, and an $e^{j\omega t}$ time variation has been assumed. The equation for curl and divergence of the incident and scattered fields can be obtained from (1) to (7) by setting $\epsilon_r = 1$ and $\sigma = 0$.

The relations between the n th-order internal and external fields at the boundary are

$$\mathbf{n} \cdot \mathbf{E}_0 = 0 \quad (8)$$

$$\hat{\mathbf{n}} \cdot \left(\sigma \mathbf{E}_n - \frac{\epsilon_r}{\eta_0} \mathbf{E}_{n-1} \right) = -\frac{\hat{\mathbf{n}}}{\eta_0} \cdot (\mathbf{E}_{n-1}^i + \mathbf{E}_{n-1}^s), \quad n \geq 1 \quad (9)$$

$$\hat{\mathbf{n}} \times \mathbf{E}_n = \hat{\mathbf{n}} \times (\mathbf{E}_n^i + \mathbf{E}_n^s) \quad (10)$$

$$\mathbf{H}_n = \mathbf{H}_n^i + \mathbf{H}_n^s \quad (11)$$

where $\hat{\mathbf{n}}$ is the outer unit normal vector at the boundary.

The zeroth-order field \mathbf{E}_0 must satisfy (1), (5), and (8), which are equivalent to the equations for the field inside a conducting ellipsoid in a uniform static electric field. The solution is $\mathbf{E}_0 = 0$. The scattered electric field \mathbf{E}_0^s is the same as the field induced by a conducting ellipsoid in a uniform static electric field. The solution for \mathbf{E}_0^s can be found by using the ellipsoidal coordinates (ξ, η, ζ) . \mathbf{E}_0^s is given by Stratton [5] as

$$\mathbf{E}_0^s = C_1 \text{grad} \left\{ [(\xi + a^2)(\eta + a^2) \cdot (\zeta + a^2)]^{1/2} \int_{\xi}^{\infty} \frac{d\xi}{(\xi + a^2)R_{\xi}} \right\} \quad (12)$$

where

$$C_1 = - \left[\sqrt{(b^2 - a^2)(c^2 - a^2)} \cdot \int_0^{\infty} \frac{d\xi}{(\xi + a^2)R_{\xi}} \right]^{-1} \quad (13)$$

and

$$R_{\xi} = [(\xi + a^2)(\xi + b^2)(\xi + c^2)]^{1/2}. \quad (14)$$

The equations for the zeroth-order scattered magnetic field \mathbf{H}_0^s and internal magnetic field \mathbf{H}_0 are equivalent to the equations for a conducting ellipsoid in a uniform magnetic field, and since the ellipsoid is nonmagnetic, the solutions are $\mathbf{H}_0^s = 0$ and $\mathbf{H}_0 = -\hat{\mathbf{z}}/\eta_0$.

As described in the prolate spheroid derivation [1], the first-order electric field, \mathbf{E}_1 will be written as the sum of two terms, $\mathbf{E}_1 = \mathbf{E}_1' + \mathbf{E}_1''$, where

$$\nabla \times \mathbf{E}_1' = 0 \quad (15)$$

$$\nabla \cdot \mathbf{E}_1' = 0 \quad (16)$$

$$\hat{\mathbf{n}} \cdot \mathbf{E}_1' = \left(-\frac{1}{\sigma \eta_0} \right) \hat{\mathbf{n}} \cdot (\mathbf{E}_0^i + \mathbf{E}_0^s) \text{ on the surface} \quad (17)$$

$$\nabla \times \mathbf{E}_1'' = \eta_0 \mathbf{H}_0 \quad (18)$$

$$\nabla \cdot \mathbf{E}_1'' = 0 \quad (19)$$

$$\hat{\mathbf{n}} \cdot \mathbf{E}_1'' = 0 \text{ on the surface.} \quad (20)$$

Since the curl and divergence of \mathbf{E}_1' are zero, \mathbf{E}_1' can be found from $\mathbf{E}_1' = \nabla \phi_1'$ where ϕ_1' satisfies Laplace's equation. In ellipsoidal coordinates, Laplace's equation is given by Stratton [5].

The properties of the ellipsoidal harmonics that satisfy Laplace's equation can be found in the literature [6], [7]. The potential ϕ_1' is an ellipsoidal harmonic which is to be found. First we will write \mathbf{E}_0^i and \mathbf{E}_0^s in terms of scalar potentials. Since $\mathbf{E}_0^i = \hat{\mathbf{x}}$, we set

$$\mathbf{E}_0^i \equiv \nabla \phi_0^i = \nabla(x) = \nabla \left[\frac{(\xi + a^2)(\eta + a^2)(\zeta + a^2)}{(b^2 - a^2)(c^2 - a^2)} \right]^{1/2} \quad (21)$$

or

$$\phi_0^i = C_2 f_1(\xi) f_2(\eta) f_3(\zeta) \quad (22)$$

with $f_i(\alpha) = (\alpha + a^2)^{1/2}$, ($i = 1, 2, 3$ and $\alpha = \xi, \eta, \zeta$), and $C_2 = [(b^2 - a^2)(c^2 - a^2)]^{1/2}$. Also, we write

$$\mathbf{E}_0^s = \nabla \phi_0^s. \quad (23)$$

From (12) and (23),

$$\phi_0^s = C_1 f_1(\xi) f_2(\eta) f_3(\zeta) \int_{\xi}^{\infty} \frac{d\xi}{f_1^2(\xi) R_{\xi}}. \quad (24)$$

From (22) and (24),

$$(\phi_0^i + \phi_0^s) = C_2 f_1(\xi) f_2(\eta) f_3(\zeta) \left[1 - \frac{\int_{\xi}^{\infty} \frac{d\xi}{f_1^2(\xi) R_{\xi}}}{A_0} \right] \quad (25)$$

where

$$A_0 = \int_0^{\infty} \frac{d\xi}{(\xi + a^2) R_{\xi}}. \quad (26)$$

The boundary condition given in (17) can be written as

$$\hat{\xi} \cdot (\nabla \phi_1') = -\frac{1}{\sigma \eta_0} [\hat{\xi} \cdot \nabla (\phi_0^i + \phi_0^s)], \quad \text{at } \xi = 0$$

or

$$\frac{1}{h_\xi} \frac{\partial \phi_1'}{\partial \xi} \Big|_{\xi=0} = \left(-\frac{1}{\sigma \eta_0} \right) \frac{1}{h_\xi} \frac{\partial}{\partial \xi} (\phi_0^i + \phi_0^s) \Big|_{\xi=0} \quad (27)$$

with

$$h_\xi = \frac{1}{2} \left[\frac{(\xi - \eta)(\xi - \zeta)}{(\xi + a^2)(\xi + b^2)(\xi + c^2)} \right]^{1/2}.$$

From (27), it can be seen that ϕ_1' must have the same η and ζ variation as $(\phi_0^i + \phi_0^s)$. We presume, therefore, that ϕ_1' is a function of the form

$$\phi_1' = C_3 g(\xi) f_2(\eta) f_3(\zeta). \quad (28)$$

Substitution of (28) into the Laplace's equation results in

$$R_\xi \frac{d}{d\xi} \left(R_\xi \frac{dg(\xi)}{d\xi} \right) - \left(\frac{b^2 + c^2}{4} + \frac{\xi}{2} \right) g(\xi) = 0 \quad (29)$$

with R_ξ given as in (14). The solutions of the preceding second-order differential equation are

$$g_1(\xi) = (\xi + a^2)^{1/2} \quad (30)$$

and

$$g_2(\xi) = (\xi + a^2)^{1/2} \int \frac{d\xi}{(\xi + a^2)R_\xi}. \quad (31)$$

Only $g_1(\xi)$ is an admissible solution for the internal potential ϕ_1' because $g_2(\xi)$ is infinite at $\xi = -c^2$ whereas $g_1(\xi)$ is finite at all points within the surface $\xi = 0$. Therefore,

$$\phi_1' = C_3 [(\xi + a^2)(\eta + a^2)(\zeta + a^2)]^{1/2}. \quad (32)$$

Substituting (32) and (25) into (27) gives

$$C_3 = -\frac{1}{\sigma \eta_0} \frac{C_2}{A_1} \quad (33)$$

with

$$A_1 = \frac{abc}{2} \int_0^\infty \frac{d\xi}{(\xi + a^2)R_\xi}. \quad (34)$$

The expression for ϕ_1' in rectangular coordinates, after substituting (33) into (32), can be written as $\phi_1' = -1/(\sigma \eta_0 A_1)x$, and then E_1' can be written as

$$E_1' = -\frac{1}{\sigma \eta_0 A_1} \hat{x} \quad (35)$$

where A_1 is given by (34).

The expression for E_1'' is found by solving (18)–(20). Since $\eta_0 \mathbf{H}_0 = -\hat{z}$,

$$\nabla \times E_1'' = -\hat{z}. \quad (36)$$

For convenience, we set

$$E_1'' = F_1 + \nabla \psi. \quad (37)$$

According to (19), then, $\nabla \cdot F_1 = 0$ and $\nabla^2 \psi = 0$. A solution of F_1 , by inspection, is $F_1 = \frac{1}{2}(y\hat{x} - x\hat{y})$. Sub-

stitution of (37) into the boundary condition given in (20) results in

$$\hat{\xi} \cdot F_1 + \hat{\xi} \cdot (\nabla \psi) = 0, \quad \text{at } \xi = 0. \quad (38)$$

The scalar potential ψ is an ellipsoidal harmonic. In addition, (38) shows that ψ must have the same η and ζ variation as F_1 . The solution for ψ in this case will have, in rectangular coordinates, the form

$$\psi = B_1 xy \quad (39)$$

which is an ellipsoidal harmonic of the second kind [7]. To find the constant B_1 , we substitute the expressions for F_1 and ψ into (38):

$$\frac{1}{2} \hat{\xi} \cdot (y\hat{x} - x\hat{y}) + B_1 \hat{\xi} \cdot (x\hat{y} + y\hat{x}) = 0, \quad \text{at } \xi = 0. \quad (40)$$

Now the unit vector $\hat{\xi}$ in ellipsoidal coordinates must be related to the unit vectors \hat{x} , \hat{y} , and \hat{z} in rectangular coordinates. This may be done by writing [8]

$$\hat{\xi} = \frac{1}{h_\xi} \frac{\partial \mathbf{r}}{\partial \xi} = \frac{1}{h_\xi} \left[\frac{\partial x}{\partial \xi} \hat{x} + \frac{\partial y}{\partial \xi} \hat{y} + \frac{\partial z}{\partial \xi} \hat{z} \right]. \quad (41)$$

Substitution of (41) into (40), after a few algebraic steps, gives $B_1 = (a^2 - b^2)/2(a^2 + b^2)$. Therefore, the final expression for E_1'' is

$$E_1'' = \frac{a^2}{a^2 + b^2} y\hat{x} - \frac{b^2}{a^2 + b^2} x\hat{y}. \quad (42)$$

Using the definition that $E_1 = E_1' + E_1''$ and the expansion series for the internal electric field, the electric field to first order inside the ellipsoid for *EKH* polarization is

$$\begin{aligned} E &= -jk(E_1' + E_1'') \\ &= -jk[(A_x + C_z y)\hat{x} + B_z x\hat{y}] \end{aligned} \quad (43)$$

where $A_x = -1/\sigma \eta_0 A_1$, $B_z = -b^2/(a^2 + b^2)$, $C_z = a^2/(a^2 + b^2)$, and A_1 is given in (34). The expression in (43) will be used for absorbed power calculation in the next section.

Expressions for E_1' , E_1'' and the internal electric field inside the ellipsoid to first order for the *EHK*, *KHE*, *KEH*, *HEK*, and *HKE* polarizations are derived by following the same procedure as described previously for *EKH* polarization. The final results for each of the aforementioned polarizations are given as follows.

B. Results for the Other Polarizations

EHK Polarization: The incident fields for this polarization are chosen to be $E^i \parallel \hat{x}$, $H^i \parallel \hat{y}$. The internal electric field to first order is

$$E = -jk(E_1' + E_1'') = -jk[(A_x + B_y z)\hat{x} + C_y x\hat{z}] \quad (44)$$

where $B_y = a^2/(a^2 + c^2)$ and $C_y = -c^2/(a^2 + c^2)$.

KEH Polarization: The incident fields are $E^i \parallel y$, $H^i \parallel \hat{z}$. The internal electric field to first order is

$$E = jk(E_1' + E_1'') = jk[(A_y + B_z x)\hat{y} + C_z y\hat{x}] \quad (45)$$

where $A_y = -1/\sigma\eta_0 A_2$, with

$$A_2 = \frac{abc}{2} \int_0^\infty \frac{d\xi}{(\xi + b^2)R_\xi} \quad (46)$$

B_z , C_z , and R_ξ are given previously.

KHE Polarization: The incident fields are $E^i \parallel \hat{z}$, $H^i \parallel \hat{y}$. The internal electric field to first order is

$$E = jk(E_1' + E_1'') = jk[(A_z + C_y x)\hat{z} + B_y z\hat{x}] \quad (47)$$

where $A_z = -1/\sigma\eta_0 A_3$, with

$$A_3 = \frac{abc}{2} \int_0^\infty \frac{d\xi}{(\xi + c^2)R_\xi} \quad (48)$$

B_y , C_y , and R_ξ are given previously.

HEK Polarization: The incident fields are $E^i \parallel \hat{y}$, $H^i \parallel \hat{x}$. The internal electric field to first order is

$$E = jk(E_1' + E_1'') = jk[(A_y + C_x z)\hat{y} + B_x y\hat{z}] \quad (49)$$

where $B_x = c^2/(b^2 + c^2)$, and $C_x = -b^2/(b^2 + c^2)$.

HKE Polarization: The incident fields are $E^i \parallel \hat{z}$, $H^i \parallel \hat{x}$. The internal electric field to first order is

$$E = -jk(E_1' + E_2'') = -jk[(A_z + B_x y)\hat{z} + C_x z\hat{y}] \quad (50)$$

The expressions for the first-order electric fields inside the ellipsoid for each of the six polarizations will be used in the next section to calculate the power absorbed by the ellipsoid.

III. ABSORBED POWER CALCULATIONS

For biological applications, it is very important to know the space density of absorbed energy rate or absorbed power, expressed in terms of watts per kilogram assuming a tissue density of 1 g/cm³.

Expressions for the first-order time-averaged specific absorbed power inside the ellipsoid is found by using the first-order internal fields given in the previous section. It should be noted here that these expressions are valid only if $\epsilon_2 \gg \epsilon_1$, which is the case of typical biological tissue at lower frequencies, ϵ_1 and ϵ_2 being the real and imaginary parts of the complex relative permittivity, respectively. The time-averaged specific absorbed power inside the ellipsoid is given by

$$P(x, y, z) = \frac{1}{2} \sigma E \cdot E^* \text{ W/m}^3 \quad (51)$$

and the space-averaged specific absorbed power is given by the volume integral

$$P_{av} = \frac{1}{V} \int_{z=-c}^c \int_{x=-a}^a \int_{-f(x,z)}^{f(x,z)} P(x, y, z) dx dy dz \quad (52)$$

where

$$f(x, z) = b \left(1 - \frac{x^2}{a^2} - \frac{z^2}{c^2} \right)^{1/2}$$

and $V = 4\pi abc/3$ is the volume of the ellipsoid.

Using the expressions for the first-order internal electric fields in (51) and (52) gives the following expressions for

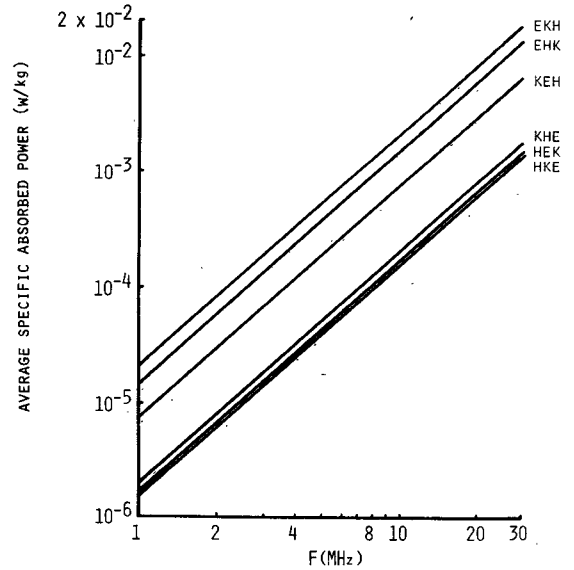


Fig. 1. Average specific absorbed power in an ellipsoidal model of man for the six standard polarizations. $a = 0.875$ m, volume = 0.07 m³, $b/c = 2.0$, $\sigma = 0.6$ mho/m a constant. Incident power density is 1 mW/cm².

the time-averaged specific absorbed power and the space-averaged specific absorbed power for the six polarizations:

$$EKH \begin{cases} P(x, y, z) = D[(A_x + C_z y)^2 + B_z^2 x^2] & (53) \\ P_{av} = D \left(A_x^2 - \frac{a^2 B_z}{5} \right) & (54) \end{cases}$$

$$EHK \begin{cases} P(x, y, z) = D[(A_x + B_y z)^2 + C_y^2 x^2] & (55) \\ P_{av} = D \left(A_x^2 + \frac{c^2 B_y}{5} \right) & (56) \end{cases}$$

$$KEH \begin{cases} P(x, y, z) = D[(A_y + B_z x)^2 + C_z^2 y^2] & (57) \\ P_{av} = D \left(A_y^2 - \frac{a^2 B_z}{5} \right) & (58) \end{cases}$$

$$KHE \begin{cases} P(x, y, z) = D[(A_z + C_y x)^2 + B_y^2 z^2] & (59) \\ P_{av} = D \left(A_z^2 + \frac{c^2 B_y}{5} \right) & (60) \end{cases}$$

$$HEK \begin{cases} P(x, y, z) = D[(A_y + C_x z)^2 + B_x^2 y^2] & (61) \\ P_{av} = D \left(A_y^2 + \frac{b^2 B_x}{5} \right) & (62) \end{cases}$$

$$HKE \begin{cases} P(x, y, z) = D[(A_z + B_x y)^2 + C_x^2 z^2] & (63) \\ P_{av} = D \left(A_z^2 + \frac{b^2 B_x}{5} \right) & (64) \end{cases}$$

where $D = \frac{1}{2} \sigma E_0^2 k^2$, E_0 is the peak value of the incident electric field, and all the other parameters appearing in (53)–(64) are given in the previous section.

Some of the power absorption characteristics are shown in the curves in Figs. 1 and 2.

Fig. 1 shows the average specific absorbed power in an ellipsoidal model of man as a function of frequency for the

six orientations. As in the case of the prolate spheroidal model, the strong orientational effect can also be seen from the figures in the ellipsoidal model. There is approximately an order of magnitude difference in average specific absorbed power between the *EKH* and *HKE* polarizations. In addition, the ellipsoidal model shows the difference in average specific absorbed power between *EKH* and *EHK*, *KHE* and *KEH*, *HEK* and *HKE* polarizations, a feature that has also been observed experimentally in measurements of the average specific absorbed power on monkeys [4]. This effect could not be predicted by the theoretical results of the prolate spheroidal model, since the prolate spheroid has a circular cross section along its major axis.

The reason for the strong dependence of average specific absorbed power on the orientation of the ellipsoid with respect to the incident electric and magnetic field vectors can be explained in terms of the electrically and magnetically induced internal fields. When the longest axis of the ellipsoid is aligned with the incident electric field, *EKH* and *EHK* polarizations, the magnitude of the internal electric field approaches that of the incident electric field because the fields are “mostly” tangential to the boundary and the boundary conditions require the tangential fields to be continuous. For the case when the incident electric field is along the shortest axis of the ellipsoid, *KHE* and *HKE* polarizations, the electric field coupling is much weaker as again expected from the field boundary conditions because, in this case, the fields are “mostly” normal to the boundary and the normal boundary conditions require the internal fields to be weaker. Therefore, the electrically induced fields can be classified as strong, intermediate, and weak for *EKH* and *EHK*, *KEH* and *HEK*, *KHE* and *HKE* polarizations, respectively. The internal electric field induced by the incident magnetic field forms loops about the incident magnetic field vector corresponding to eddy currents, and the strength of this magnetically induced electric field appears to be in some sense proportional to the ellipsoidal cross-sectional area perpendicular to the incident magnetic field. Thus strong magnetic coupling occurs when the incident magnetic field vector is along the shortest axis of the ellipsoid. *KEH* and *EKH* polarizations. The magnetically induced fields can also be classified as strong, intermediate, and weak for *EKH* and *KEH*, *EHK* and *KHE*, *HEK* and *HKE* polarizations, respectively.

From the foregoing discussion, one would expect the average specific absorbed power to be the greatest for the *EKH* polarization because both electric and magnetic field coupling are strong, and the average specific absorbed power for *HKE* polarization to be the smallest because both electric and magnetic coupling are weak. This is indeed the case as shown in Figs. 1 and 2. The intermediate steps in terms of absorbed power, *EHK*, *KEH*, *KHE*, and *HEK* polarizations, are the result of the various combinations of electric and magnetic coupling.

Fig. 2 illustrates the normalized average specific absorbed power in an ellipsoidal model of man for each polarization, as a function of b/c . It is interesting to note that the average specific absorbed power, for the *EKH* and *KEH* polariza-

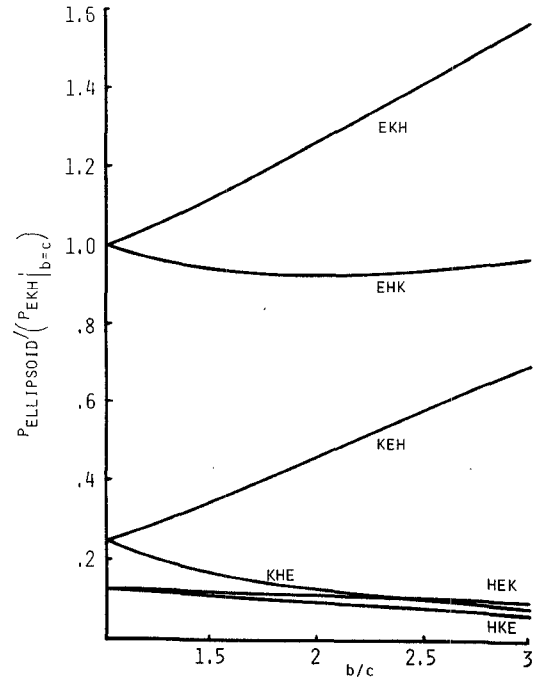


Fig. 2. Relative absorbed power in ellipsoids as a function of polarization and b/c . $a = 0.875$ m, volume = 0.07 m³, frequency = 10 MHz, $\sigma = 0.6$ mho/m.

tions, increases as the b/c ratio increases. This occurs because the increase in b/c ratio has two effects. The first is that the cross-sectional area normal to the incident magnetic field increases, for the two polarizations, causing an increase in the strength of the magnetically induced E field. The second effect is that an increase in the b/c ratio thins out the ellipsoid and makes it less shielded from the incident E field and therefore produces a strengthened electrically induced E field, specially for the *EKH* polarization. For $b/c = 1$, the ellipsoid takes the shape of a prolate spheroid, and for this value of b/c the results of the calculations of absorbed power in ellipsoids are the same as those previously obtained for a prolate spheroid having the same volume and the same height as the ellipsoid [1].

Theoretical results have also been obtained for the ellipsoidal model of a sitting monkey, with good qualitative agreement with measurements of power absorbed by live monkeys made at Brooks Air Force Base [4]. The relatively good qualitative agreement between the theoretical and experimental data indicates that the ellipsoid is a better model for some experimental animals and man than the prolate spheroid.

A better quantitative agreement between the theory and experiment might be achieved by choosing the optimum combination of the dimensions of the ellipsoidal model, a , b , and c , and the electrical properties of the model to best fit the animal data.

IV. SUMMARY AND CONCLUSIONS

The first-order internal electric fields and specific absorbed power in ellipsoidal models of man and experimental animals irradiated by an EM plane wave have been obtained

for the case when the wavelength is long compared to dimensions of the ellipsoid $a/\lambda < 0.1$. The expressions for the internal fields and specific absorbed power, and the curves of specific absorbed power versus frequency, show that the internal electric fields and the specific absorbed power depend on the body's dielectric properties and geometry, as well as the frequency and polarization of the incident wave.

Comparison of the theoretical specific absorbed power in prolate spheroidal and ellipsoidal models with the corresponding experimental data on live monkeys indicates that the prolate spheroidal models are not adequate for primates, although they may be for rodents since their cross sections taken normal to the long axis appear to be approximately circular. However, for primates, with approximately elliptical cross sections, the ellipsoidal model would obviously be a superior representation.

The expressions for the internal electric fields, specific absorbed power, and space-average specific absorbed power should prove to be very valuable in studies of radiation hazards to man for the long-wavelength case. A very important application of this analysis will be in the extrapolation to man of the results of animal experiments involving biological effects due to EM radiation. Since the results of this analysis show marked differences in EM absorption characteristics for man compared to that of animals at the same frequency and same incident field level, in extrapolating animal effects to man it will be necessary to relate the biological effects to the internal fields or power absorption and then relate the internal fields or power absorption to the incident fields.

In a future communication, we will apply this analysis to obtain data showing the internal specific absorbed power distribution and average specific absorbed power in different test animals and different human body types.

APPENDIX

The constants A_1 , A_2 , and A_3 occurring in (34), (46), and (48) are related to semiprincipal axes of the ellipsoid a , b , and c , and to the incomplete elliptic integrals of the first and second kinds [9]. These relations are as follows:

$$A_1 = abc \left(\frac{[F(\phi, k) - E(\phi, k)]}{[(a^2 - b^2)(a^2 - c^2)^{1/2}]} \right) \quad (A1)$$

$$A_2 = abc(a^2 - c^2)^{1/2} \cdot \left[\frac{[E(\phi, k) - (b^2 - c^2)F(\phi, k)/(a^2 - c^2) - ak^2 \sin \phi \cos \phi/b]}{[(a^2 - b^2)(b^2 - c^2)]} \right] \quad (A2)$$

$$A_3 = abc \left[\frac{[b \tan \phi/a - E(\phi, k)]}{[(b^2 - c^2)(a^2 - c^2)^{1/2}]} \right] \quad (A3)$$

with

$$F(\phi, k) = \int_0^\phi (1 - k^2 \sin^2 \theta)^{-1/2} d\theta \quad (A4)$$

$$E(\phi, k) = \int_0^\phi (1 - k^2 \sin^2 \theta)^{1/2} d\theta \quad (A5)$$

and

$$k = \left(\frac{a^2 - b^2}{a^2 - c^2} \right)^{1/2} \quad (A6)$$

$$\phi = \sin^{-1} \left(\frac{a^2 - c^2}{a^2} \right)^{1/2} \quad (A7)$$

where $F(\phi, k)$ and $E(\phi, k)$ are the incomplete elliptic integrals of the first and the second kinds, respectively. In this Appendix we made use of the customary symbol k for modulus of these elliptic integrals, and it should not be confused with the parameter k used for the free-space propagation constant in the main body of this paper. It can be shown that the order of the relative magnitude of the constants A_1 , A_2 , and A_3 is the inverse of the order of the three parameters a , b , and c . That is, if $a > b > c$, then $A_1 < A_2 < A_3$. Furthermore, one finds that $A_1 + A_2 + A_3 = 1$.

REFERENCES

- [1] C. H. Durney, C. C. Johnson, and H. Massoudi, "Long-wavelength analysis of plane wave irradiation of a prolate spheroidal model of man," *IEEE Trans. Microwave Theory Tech.*, vol. MTT-23, pp. 246-253, Feb. 1975.
- [2] C. C. Johnson, C. H. Durney, and H. Massoudi, "Long-wavelength electromagnetic power absorption in prolate spheroidal models of man and animals," *IEEE Trans. Microwave Theory Tech.*, vol. MTT-23, pp. 739-747, Sept. 1975.
- [3] O. P. Gandhi, "Frequency and orientation effects on whole animal absorption of electromagnetic waves," *IEEE Trans. Biomed. Eng. (Commun.)*, vol. BME-22, pp. 536-542, Nov. 1975.
- [4] S. J. Allen, W. D. Hurt, J. H. Krupp, J. A. Ratliff, C. H. Durney, and C. C. Johnson, "Measurement of radio frequency power absorption in monkeys, monkey phantoms and human phantoms exposed to 10-50 MHz fields," *Proc. 1975 Annual USNC-URSI Meeting*, Boulder, CO, p. 200, Oct. 1975.
- [5] J. A. Stratton, *Electromagnetic Theory*. New York: McGraw-Hill, 1941.
- [6] E. T. Whittaker and G. N. Watson, *A Course of Modern Analysis*, New York: Macmillan, 1946.
- [7] P. M. Morse and H. Feshbach, *Methods of Theoretical Physics*, Part II. New York: McGraw-Hill, 1953.
- [8] M. R. Spiegel, *Mathematical Handbook of Formulas and Tables* (Schaum's Outline Series). New York: McGraw-Hill, 1968, p. 124.
- [9] P. F. Byrd and M. D. Friedman, *Handbook of Elliptic Integrals for Engineers and Scientists*, 2nd Edition, Revised. New York, Heidelberg, Berlin: Springer-Verlag, 1971.